Journal of Volcanology and Geothermal Research 174 (2008) 257–268

Contents lists available at ScienceDirect

Journal of Volcanology and Geothermal Research

journal homepage: www.elsevier.com/locate/jvolgeores

Geophysical imaging of buried volcanic structures within a continental back-arc basin: The Central Volcanic Region, North Island, New Zealand

W.R. Stratford [a,b,*], T.A. Stern [a]

[a] Institute of Geophysics, Victoria University of Wellington, New Zealand
[b] Institute of Geology, University of Copenhagen, Denmark

ARTICLE INFO

Article history:
Received 20 September 2007
Accepted 27 February 2008
Available online 15 March 2008

Keywords:
refraction seismology
Central Volcanic Region
calderas
New Zealand tectonics
continental back-arc
andesite arc
gravity anomalies

ABSTRACT

Hidden beneath the ~2 km thick low-velocity volcaniclastics on the western margin of the Central Volcanic Region, North Island, New Zealand, are two structures that represent the early history of volcanic activity in a continental back-arc. These ~20×20 km structures, at Tokoroa and Mangakino, form an adjacent gravity high and low, respectively. Interpretations from seismic refraction arrivals and gravity modelling indicate the −65 mgal Mangakino residual gravity anomaly can be modelled, in part, by two low-density bodies that reach depths of ~6.5 km, whereas the Tokoroa gravity anomaly is due to a higher density rock coming, at most, to within ~650 m of the surface. The Mangakino anomaly is interpreted to be due to the remnants of magma chambers that fed large ignimbrite eruptions from about 1.2 Ma. An andesite volcano or complex volcanic structure is the preferred interpretation for the Tokoroa gravity high. The size of the putative volcanic structure is comparable to the presently active Tongariro Volcanic Complex in the centre of North Island.

1. Introduction

Volcanism produced above and behind active continental margins can contain the full spectrum of eruptive volcanic compositions, from basaltic to rhyolitic. Andesite volcanoes are the iconic manifestations of an active subduction zone, but after subduction is established rhyolitic volcanism can develop and basalts may also be present, albeit in lower abundance (Hamilton, 1995). In addition, continental back-arcs that have become evolved, like the western USA, develop late stage hi-K volcanism that is now interpreted to be linked to convective removal of mantle lithosphere (Farmer et al., 2002). In trying to decipher the plate tectonic history of any given margin knowledge of the type of volcanism is, therefore, important.

It is also important to know how any particular volcanic rock-type is distributed in time and space. For example, dating of volcanic rocks and palaeomagnetism has led to a better understanding of continental back-arc evolution in both Japan and the Mediterranean. At both these localities rapid rotation of the active volcanic arc and fan-shaped openings have been proposed (Faccenna et al., 2001). A similar, fan-like opening has been proposed for the Central Volcanic Region (CVR) of New Zealand, based on andesite ages, GPS and paleomagnetic data (Calhaem, 1973; Stern, 1987).

One of the major hindrances to identification of past arcs and caldera structures behind active continental margins is that the volume and extent of rhyolitic deposits, including ignimbrites, are so vast and thick that many of the older volcanic structures are now buried. However, andesite, rhyolite and basalt volcanic rocks have contrasting geophysical properties (Murase and McBirney, 1973) and therefore geophysical methods have the potential to explore and map beneath the thick layers of volcaniclastics that smother the central North Island. In this study we concentrate on some large geophysical anomalies near the western boundary of the CVR. We apply seismic and gravity methods to try and identify volcanic structures beneath thick volcaniclastic layers, and interpret the structure within the context of some dynamic models. Relative delays of low-frequency refraction arrivals are the principal method used here to gain constraints on the distribution of volcaniclastic material within the top few kilometres of the crust.

2. Volcanic/tectonic setting of North Island, New Zealand

Subduction related andesitic volcanism began in the North Island around 27 Ma (Issac et al., 1994). Even before the volcanics were precisely dated it was recognised that there is an apparent south and eastward progression of low-potash andesites through the northern and central North Island from the early Miocene (Hatherton, 1969). Upon the availability of K/Ar dates a temporal migration could be quantified (Calhaem, 1973). In Northland, andesite volcanism existed

* Corresponding author. Present address: Institute of Geology, University of Copenhagen, Denmark.
E-mail address: ws@geol.ku.dk (W.R. Stratford).

0377-0273/$ – see front matter © 2008 Elsevier B.V. All rights reserved.
doi:10.1016/j.jvolgeores.2008.02.011

from 27–16 Ma, followed by activity in the Coromandel region (17–5 Ma) with a final move to the CVR in the last 4–5 My (Fig. 1).

Evidence for a ~6°/My fan-like extension for the CVR comes from a range of long (My) and short (decade) term proxies: palaeomagnetism (Wright and Walcott, 1986); geological studies (Stoneley, 1968; Cole and Lewis, 1981); the apparent migration of volcanic arcs inferred from the distribution of dated andesites (Calhaem, 1973; Stern et al., 2006) (Fig. 1) and GPS (8–15 mm/yr) (Wallace et al., 2004). A more recent model includes rotation and extension in the central North Island, at rates of about 3°/My, combined with vertical axis rotations of eastern North Island (Nicol et al., 2007). A different concept is that there were just two linear volcanic arcs; one Miocene, orientated near north–south, and one Quaternary orientated NE–SW (Wilson et al., 1995), and the transformation from one arc to another is proposed to be achieved in one discrete movement. The apparent hinge point for such a discrete step occurs in the Mangakino–Tokoroa region of the CVR (Figs. 1 and 2) where this study is focussed.

Between 5 and 2 Ma the volcanic arcs in North Island, and much of the east coast fore-arc basin (Fig. 1), can be interpreted to have translated and rotated from the ~340° azimuth of the Coromandel Volcanic Zone arc to the ~40° azimuth of the Taupo Volcanic Zone arc (King, 2000) (Fig. 1). Specific arc positions within the 5–2 Ma period are still poorly understood as the onshore arc is of limited extent and there are only a few andesite peaks available to date and delineate the volcanic front (Stern et al., 2006). Moreover, a recent andesite date from Motiti Island (Fig. 1) serves to broaden the 5–2 Ma transition zone (Briggs et al., 2006). The Motiti Island age appears to be an outlier with respect to the other dates for reasons which are unknown. Nevertheless, a transition region between the Miocene and Pliocene andesite arcs lies in the northwest corner of the CVR, and along its western margin, just to the north of the Mangakino–Tokoroa region (Fig. 2).

Extension is manifest behind the Coromandel arc in the ~10–0 Ma Hauraki rift (Hochstein and Ballance, 1993), and behind the Taupo arc in the extended crust of the wedge shaped CVR. These two extensional regions merge and overlap at the northwestern corner of the CVR. Back-arc rhyolitic activity started at the north end of the Coromandel Volcanic Zone at ~12 Ma (Skinner, 1986) and progressed south-eastward with time. Active rhyolite volcanism is now confined to the Taupo Volcanic Zone (TVZ) (Fig. 1) (Cole et al., 1995). The present day andesite arc defines the eastern boundary of the Taupo Volcanic Zone. The TVZ includes the volcanically and geothermally active part of the CVR, encompassing recognised rhyolite caldera structures less than 2 Ma (Figs. 1 and 2) (Cole et al., 1995).

2.1. Setting of the Mangakino–Tokoroa area

Steep gravity gradients define the western and eastern edges of the CVR. The basement surface of the region has subsided by ~2 km (Stern, 1986; Horgan, 2003) and the region has a background residual gravity anomaly of −40 mgals (Fig. 2). Two of the most prominent features of the CVR subsurface, as inferred from the residual gravity field, are the Mangakino Caldera (Wilson et al., 1995; Krippner et al., 1998) and the Tokoroa gravity high (Fig. 2). Their residual gravity anomalies are a significant departure from the overall background level of the volcanic area; a minimum −65 mgals over the Mangakino Caldera, and maximum −15 mgals associated with the Tokoroa gravity high (Fig. 2).

Although the Mangakino area was flooded by a hydroelectric scheme in the 1950's (Healy et al., 1964), a number of recent temperature measurements taken in a ~3 km deep drill hole near Mangakino reveal elevated temperatures within the caldera (Spinks et al., 2005). The elevated temperatures and a shallow depression are the only surface measurable evidence of the structure beneath, as the caldera has largely been filled with younger volcanic and lacustrine deposits (Grindley and Mumme, 1991).

Early geological mapping in the area identified the Mangakino Caldera as the source, and prolific producer, of a large thickness of the earliest ignimbrites erupted from the CVR (Blank, 1965). Dating of ignimbrite sheets indicates the onset of sialic volcanism in the caldera occurred at ~1.60 Ma (Wilson, 1986; Briggs and McDonough, 1990). This activity is almost contemporaneous with the youngest rhyolite volcanism of the Coromandel Volcanic Zone dated at ~2 Ma (Skinner, 1986). Thus, in a geological time frame, the switch from Coromandel Volcanic Zone to CVR rhyolitic activity is rapid and possibly continuous as has been postulated by others (Carter et al., 2003).

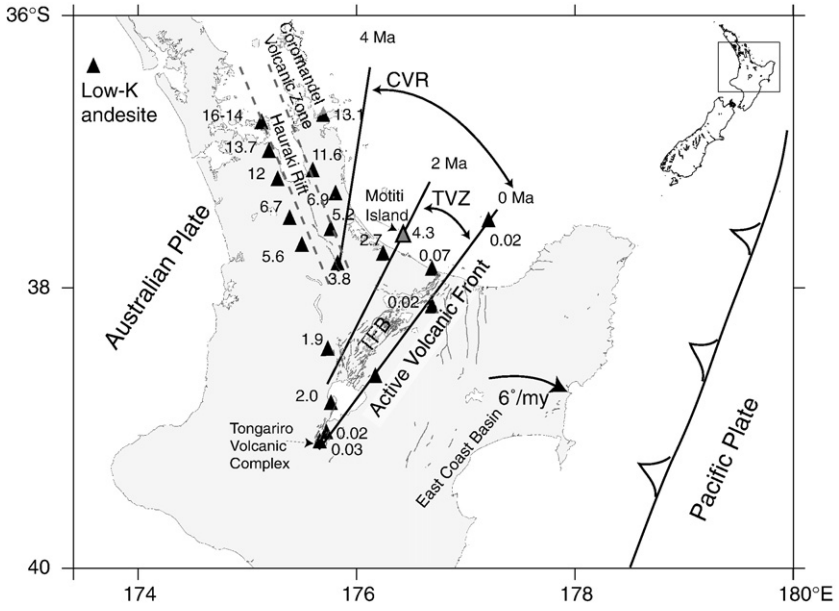

Fig. 1. Location map of the central North Island, New Zealand. Positions of the low-K andesites of the central North Island. The present day Active Volcanic Front is labelled. There is an apparent migration of the low-K andesites both south and east across the island. Andesite K/Ar dates from Stipp and Thompson (1971), Briggs (1986) and Skinner (1986). Motiti Island andesite (grey triangle) age from Briggs et al. (2006). Rotation rate of the eastern North Island from Wright and Walcott (1986) based on paleomagnetic data from the East Coast Basin. The figure shows the locations of the Coromandel Volcanic Zone, the Hauraki Rift, the Central Volcanic Region (CVR) and the Taupo Volcanic Zone (TVZ). The grey lines within the TVZ are the fault segments of the Taupo Fault Belt (TFB).

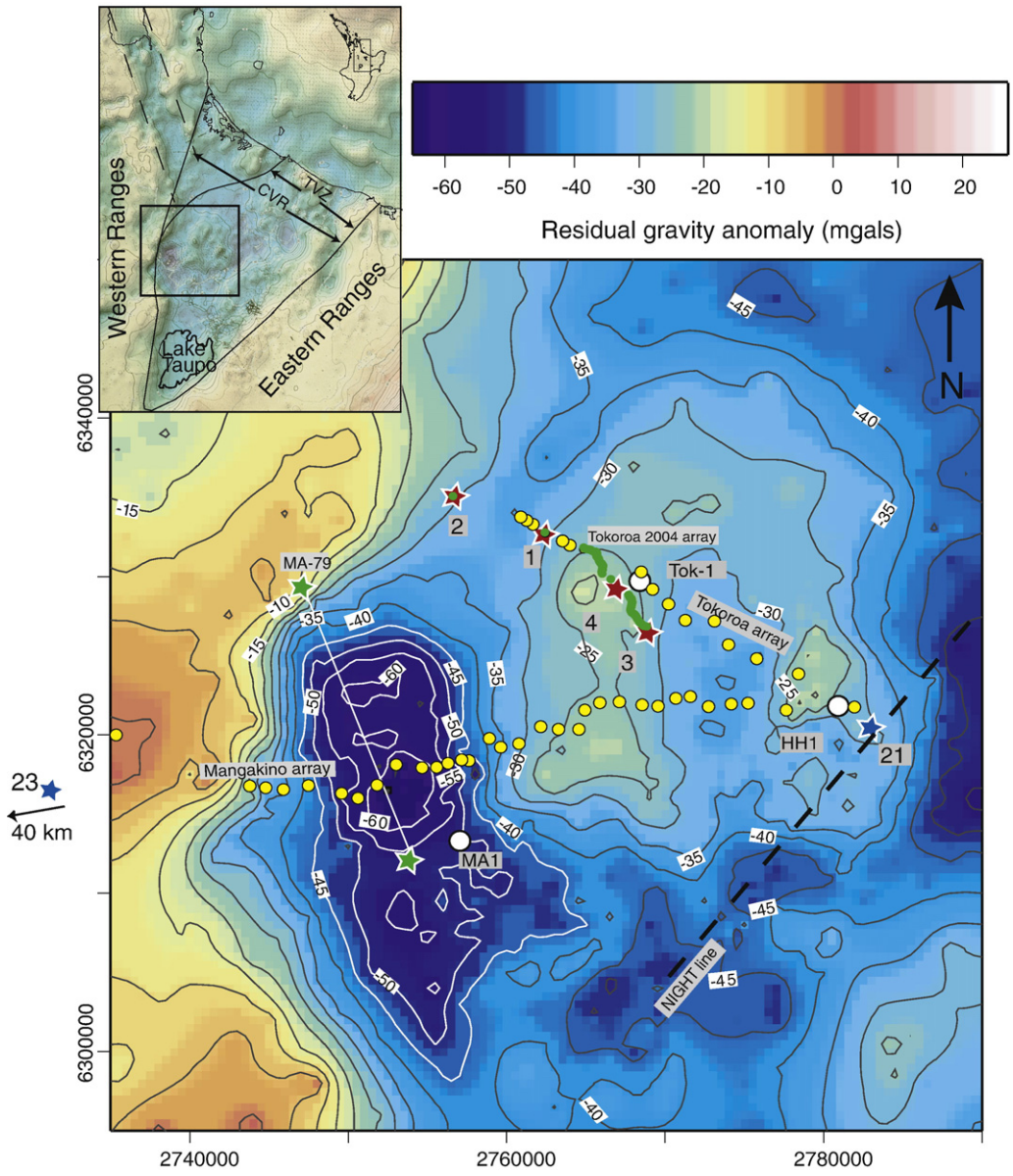

Fig. 2. Residual gravity anomaly of the Tokoroa and Mangakino areas derived by method described by Stern (1979). Colour bar shows values of residual anomaly from −65 to 20 mgals. Yellow dots are the receiver locations of the Tokoroa and Mangakino arrays, and green dots and green lines are the receiver locations of the Tokoroa-2004 seismic array. The numbers refer to shot gathers in other figures in this document. The Tokoroa and Mangakino gravity profiles (Fig. 9) run along the seismic lines. Three drill holes in the area used for lithology information and densities are marked as white dots (MA1, Tok-1 and HH1). Black line shows the extent of the ~North–South NIGHT line in this area. MA-79 is previous North-South seismic line (Stern, 1982). Co-ordinates are in metres in New Zealand Map grid. Inset: Residual gravity map of the CVR (Institute of Geological and Nuclear Sciences, geophysical maps: 13). Yellow areas on edges ~0 mgal and the overall blue back ground level for the triangular shaped CVR is ~−40 mgals.

The structure producing the Tokoroa gravity high has no surface expression (Fig. 2) and was first discovered with geophysical methods (Stern, 1979; Rogan, 1982). How the Tokoroa structure relates to the volcanic setting of the western margin of the CVR is still in contention. There are two possibilities: the structure could represent a block of basement greywacke that subsided from the western margin (Rogan, 1982), or a buried andesite volcano of similar size to the Tongariro Volcanic Complex at the southern tip of the CVR (Fig. 1).

3. Previous work

Seismic investigations in the Mangakino region in the late 1970's included a north–south orientated, and reversed, seismic line (Fig. 3) (Stern, 1982). This line (MA-79 in Fig. 2) provides velocity information perpendicular to the east–west orientated Mangakino array presented in this paper. A "seismic basement" of velocity 4.8±0.2 km/s was detected at a depth of 2.2±0.2 km (Stern, 1982). Above seismic basement are low-velocity volcaniclastics ranging in P-wave speed from 1.2–3.2 km/s (Fig. 3) and a ~45° dipping margin at the north end of the profile. Such a thickness of low-velocity, and hence low-density, rock can only account for about −40 mgals of the observed −65 mgal residual anomaly. There is still a −25 mgal second-order residual to explain. One proposed explanation is a deep reaching (~6 km) body of density contrast −320 kg/m^3, relative to basement, with a 10 km strike-length in a north–south direction (Stern, 1986).

A physical interpretation of such a deep reaching low-density body is unclear. Density data from boreholes indicates that most of the porosity, and hence density contrast, of volcaniclastics collapses with a depth of

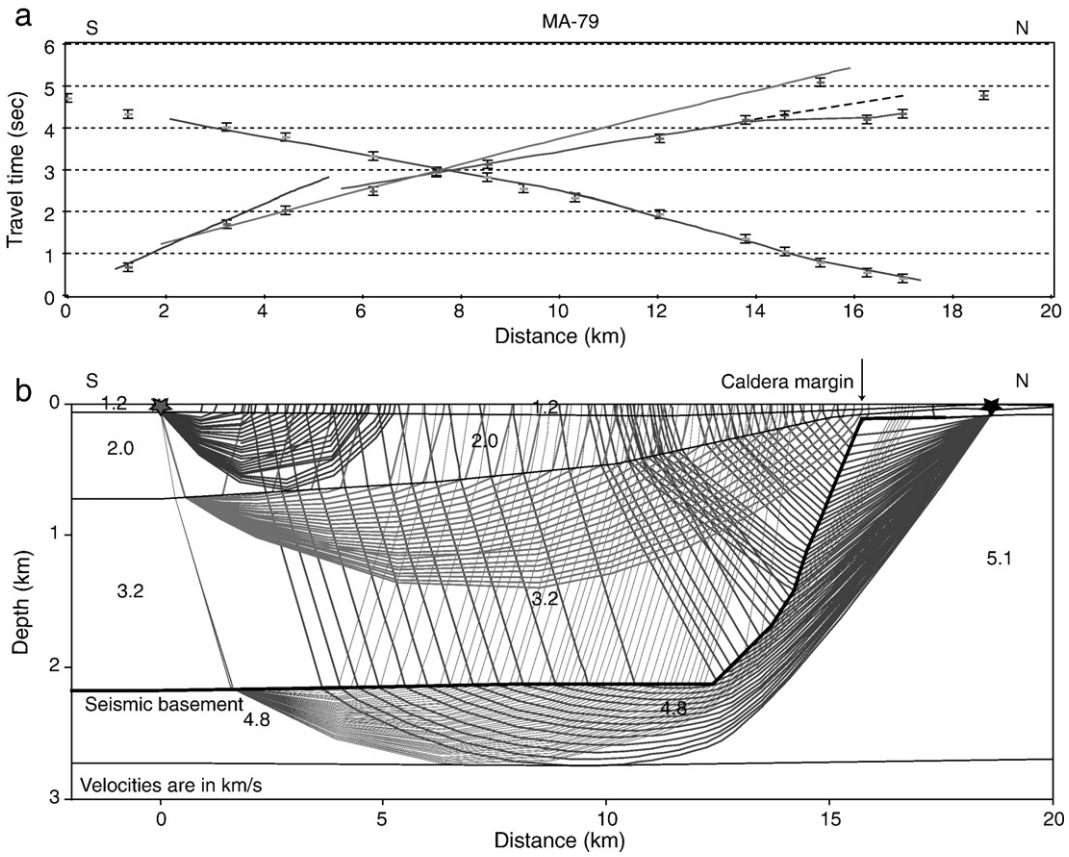

Fig. 3. Seismic velocity and ray tracing model for the North–South line through Mangakino Caldera. Ray-tracing structure derived using original analogue data (Stern, 1982). Shot points and a profile line for the seismic array are labelled on Fig. 2 (green stars). a.) Travel time picks for arrivals from the north and south shots. The lines represent model fits to the picks. b.) Interpreted velocity structure for the north–south seismic line. Average layer velocities are shown.

burial of about 2.5 km (Stern, 1986) (Fig. 7). Thus the interpretation of the deep reaching low-density body beneath Mangakino calls for some active process to maintain the low densities to depths of 6 km.

Previous work in the Tokoroa area included a number of seismic refraction profiles used here to constrain the near surface velocities. An average surface layer velocity of 1.5 km/s for the top 100 m (Alder, 1989) is used for modelling both the Tokoroa and Mangakino regions. A previous 3D gravity model of the Tokoroa gravity high (Alder, 1989) is also used as a starting reference point for modelling the structure.

4. Seismic surveying

4.1. Field and interpretation methods

In 2001, two 25–35 km-long seismic arrays were deployed to investigate the Mangakino Caldera and Tokoroa gravity high (Fig. 2). These arrays were shot as part of the NIGHT (North Island GeopHysical Transect) crustal structure project (Henrys et al., 2003). Additional data from NIGHT are used to constrain the velocity structure of the western North Island (Fig. 2) and seismic basement velocities beneath the Mangakino and Tokoroa arrays. Arrivals from shot 21 were recorded on the main NIGHT array over the eastern edge of the Tokoroa gravity high (Stratford and Stern, 2006) (Fig. 2). The NIGHT array runs roughly northeast–southwest and perpendicular to the Tokoroa and Mangakino arrays. In this northeast–southwest direction the gravity signature of the Tokoroa high is relatively flat. A basement velocity of 4.8±0.2 km/s is interpreted with data from the NIGHT array (see Stratford and Stern, (2006)), which is the same as that found beneath the MA-79 profile (Fig. 3) and is therefore adopted as the "seismic basement" velocity for the Tokoroa and Mangakino region.

The Tokoroa and Mangakino arrays consist of 18 and 34 seismographs, respectively, at ~1 km spacing (Fig. 2). The east–west Mangakino array is reversed by shots 21, and shot 23 in the western North Island, and the northwest orientated Tokoroa array is end-shot by shot 21 at its southeast end (Fig. 2). Both shots were 500 kg in charge size and were shot in 50 m deep boreholes. As a partial reversal of the Tokoroa array, additional seismic data were collected in 2004 along two, 2 km-long arrays with four 50 kg shots (shots 1–4) fired along a short section at the western end (Fig. 2). At this western end of the array the gravity anomaly reaches a local maximum, and therefore the causative body is assumed to be closer to the surface.

Subsurface relief beneath the Mangakino and main Tokoroa seismic profiles is indicated by undulating first arrival travel times (Figs. 4 and 5). Such undulations make linear regression analysis for the layer velocities beneath the profiles inappropriate. Instead, forward modelling is used to model the subsurface layer depths and velocity variations, and reproduce refraction travel times.

4.2. Mangakino array

From shot 21 on the Mangakino array, undulations in the first arrival times are observed over the western edge of the Tokoroa gravity high at offsets of 0–28 km (Fig. 4). Relative travel time delays of ~0.85 s, associated with variations in the thickness of volcanic fill within the Mangakino Caldera, are observed at offsets of 28–35 km. But the most notable feature of these data is the double arrival for waves that have traversed beneath the caldera: a weak first arrival with an apparent Vp of 5.0±0.2 km/s and, delayed 0.4 s behind this, a higher amplitude second arrival with an apparent Vp of 4.6±0.2 km/s (Fig. 4b). Significantly, these second arrivals are observed from the

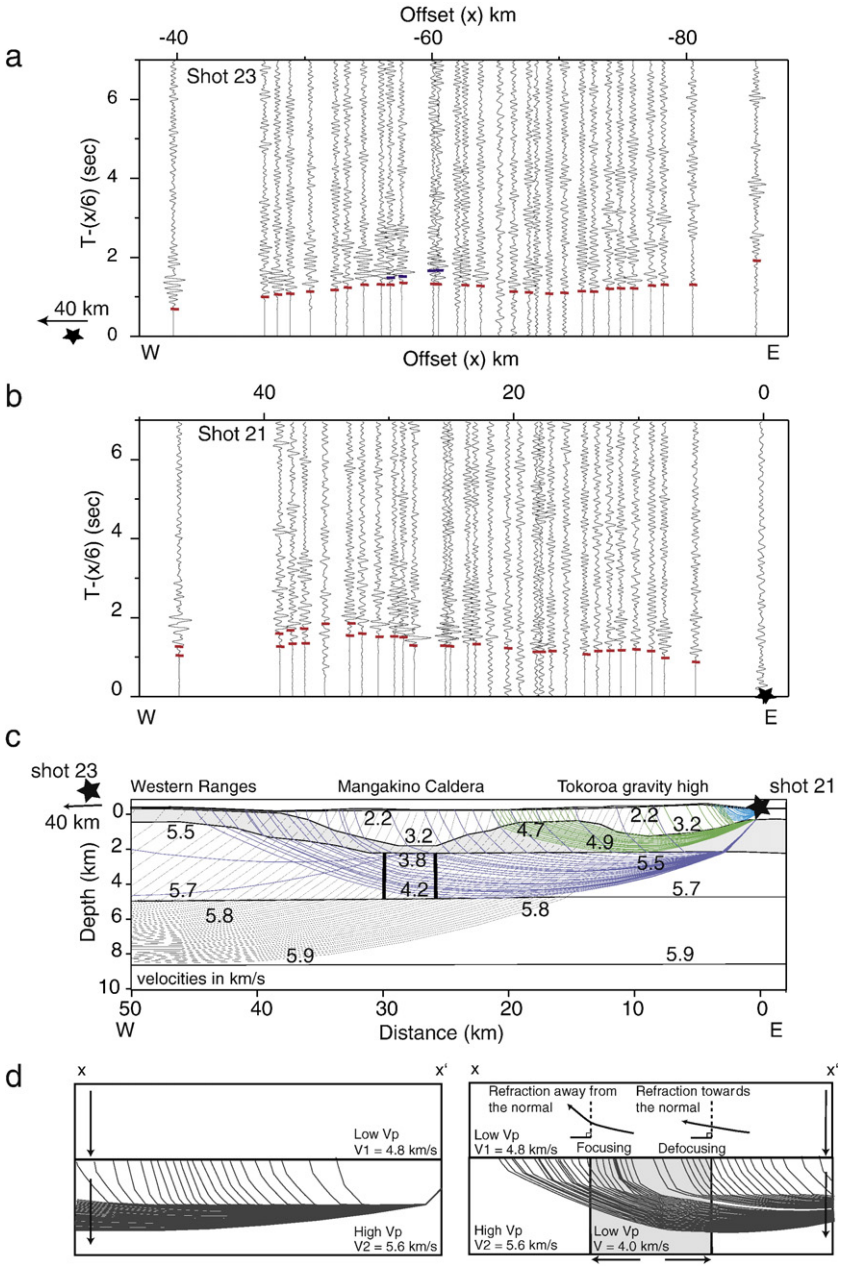

Fig. 4. a,b). Mangakino profile seismic data, shots 23 (a) and 21 (b). Data are shown at reduced travel time $t=T-(x/6)$. Where x=offset, T=absolute travel time and t=reduced travel time. Offsets are relative to shot point locations, and positive to the west. Note the undulation in first arrivals times and the relatively high-amplitude second arrivals at far offsets on shot 21. The reversal of this arrival is tentatively marked on shot 23. c.) Ray-tracing model for the Mangakino array. Top and bottom velocities for each layer are shown; there is a continuous gradient between these values. A low-velocity body, between offsets of 25–30 km and with Vp=~4.0 km/s, is modelled beneath Mangakino Caldera. Absolute depth of the low-velocity body beneath the caldera is not well constrained by the seismic data. Positions of the Western Ranges, Mangakino Caldera and Tokoroa gravity high are shown. d.) Ray paths for seismic propagation through horizontally homogeneous layers (with vertical velocity gradients) (left), and seismic energy incident on a low-velocity body at depth (with additional horizontal velocity gradients) (right). Arrows show directions of velocity increase. The x–x' distance is the 22–34 km offset range in c.) Waves are refracted towards the normal and defocused passing laterally from a high Vp to a low-Vp layer. Passing from the low-Vp body into the higher velocity country rock waves are refracted away from the normal to the vertical interface, focusing occurs and amplitudes are increased.

centre and to the west of the centre of the caldera, as defined by the closed contours of the −60 mgal gravity contour (Fig. 2).

Undulating first arrivals are also recorded from shot 23 (to the west) and similar second arrivals from beneath the caldera are seen. However, these second arrivals are less clear than on shot 21 (Fig. 4a).

4.2.1. Forward modelling solution — Mangakino array

Travel times for shot 21 recorded on the Mangakino array are fitted by varying the depth to "seismic basement" or the 4.8±0.2 km/s refractor (Fig. 4c). A seismic basement high that shallows to ~750 m below the surface is modelled over the southwestern flank of the Tokoroa gravity high (Fig. 4c). Within the caldera seismic basement is at 2.1±0.1 km, which is in accord with the earlier Mangakino refraction experiment (Stern, 1982) (Fig. 3).

The slower, higher amplitude second arrivals through the caldera (shot 21, Fig. 4b) are a puzzling feature, especially as the caldera is known for its high attenuation of seismic waves (Salmon et al., 2004). This phenomenon is attributed to focussing of rays passing through an inferred low-Vp body, which is modelled with an average velocity of

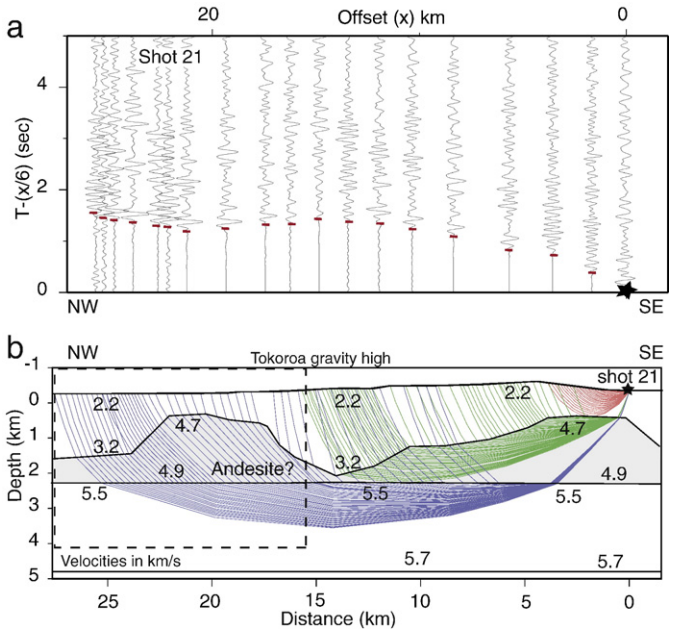

Fig. 5. a.) Tokoroa seismic data from shot 21. Offsets are relative to the shot location (see Fig. 2) and positive to the west. Data are shown in reduced travel time as in Fig. 4. b.) Ray-tracing model for the Tokoroa line. Top and bottom layer velocities are shown with linear gradient of velocity between. Grey shading is the inferred causative body of the Tokoroa gravity high. The dashed box shows the region covered by the Tok-2004 seismic array (Fig. 6).

~4.0 km/s (Fig. 4c). The average velocity of the body (V_1) can be estimated from

$$V_1 = (\partial t/x + 1/V_2)^{-1} \quad (1)$$

Where ∂t is the difference in travel times between the first and second arrivals, x is the path length of waves through the body and V_2 is the first arrival velocity of 5.6 km/s. For $\partial t = 0.3$ s, $V_2 = 5.6$ km/s and a slant ray path (x) of length 4.5 km, Eq. (1) gives a velocity for the anomalous body (V_1) of 4 km/s.

Weak first arrivals through the caldera from shot 21 at offsets of 28–35 km (Fig. 4b) are interpreted as refracted arrivals through a 5.6± 0.2 km/s crustal layer. These arrivals appear to be unaffected by the low-velocity (low-density) body beneath the Mangakino Caldera and are interpreted to "sideswipe" the structure or penetrate through it via a section of more competent rock.

Alternative models where the second arrivals are produced by variations in the near surface velocity structure have been explored but are dismissed as they cannot reproduce the observed spatial pattern of the observed second arrival travel times.

The north–south seismic refraction array (Fig. 3) shows that towards the centre of the caldera there is an increase in thickness of the low-Vp rock (~2–3 km/s) to ~750 m (Fig. 3) (Stern, 1982). To reproduce the magnitude of the delay between the first and second arrivals on the Mangakino seismic line a low-Vp layer (~2 km/s) ~1 km thick is required. Moreover, the second arrivals are observed west of the caldera centre and to produce such delayed arrivals at the observed location requires the boundaries of the caldera to be shifted 5 km further west. This is not feasible as the western edge of the caldera is well defined by its gravity signature (Fig. 2) and an alternative explanation is required.

4.2.2. Focussing and amplitude effects in a low-Vp body beneath Mangakino Caldera

The low-velocity body beneath Mangakino Caldera is modelled with vertical and lateral velocity gradients, grading from higher velocities at the edges to lower velocities in the centre. The effect of lateral velocity gradients can be predicted by applying Snell's law (Sheriff and Geldart, 1995). Passing laterally from a low-velocity rock into the higher velocity country rock waves are refracted away from the normal to the vertical interface (Fig. 4d). Focusing occurs and there is a higher ray density (larger amplitude) above the far side of, and just outside, the low-density rock. This is what appears to be observed (Fig. 4b): i.e. the most prominent, delayed, high-amplitude phase is mainly detected west of the centre of the caldera much like a shadow effect. Likewise, shooting from the west (Fig. 4a) there are late arrivals spread above and east of the deep caldera, low-velocity body.

The second arrivals from beneath the caldera are, therefore, interpreted as turning waves through the 5.6 km/s layer that are then channelled along a slanted path through a ~4 km/s low-velocity body, which extends to depth beneath the caldera.

4.3. Tokoroa arrays

Along the Tokoroa array first arrivals are identified with a large variation in amplitude (Fig. 5a). The general increase in amplitude at offsets greater than 20 km is likely to be due to focussing effects (Sheriff and Geldart, 1995) associated with the rays passing laterally out of a higher velocity subsurface body into lower velocity volcaniclastics (Fig. 5b). Arrivals interpreted to be from seismic basement are recorded at offsets greater than 3.5 km with an apparent Vp of 4.8±0.2 km/s (Fig. 6b). First arrivals from a deeper basement interface with a Vp of 5.6 km/s are recorded at offsets greater than 10 km (Figs. 4 and 5). Although the Tokoroa line is only partially reversed, and the model presented is non-unique, confidence is given by a similar suite of velocities being modelled beneath the reversed Mangakino array (Fig. 4c).

4.3.1. The Tokoroa gravity high

Relief on the seismic basement structure beneath the Tokoroa array is interpreted as "basement" highs under the east and west ends of the line separated by a central low (Fig. 5b). The top of the western high, at offsets of 15–25 km (Fig. 5b), is further constrained by the Tokoroa-2004 data to be 0.65±0.1 km below the surface (Fig. 6). From the slopes of the first arrivals on the Tok-2004 shot gathers, four layers are distinguished (Fig. 6). Extreme relief on the edge of the Tokoroa structure is supported by the observed high apparent velocities of layer three (Vp=11 km/s from shot 1).

5. Structural interpretations from gravity data

Residual gravity anomalies for the CVR are defined by removing a regional field. For the CVR a regional field is calculated by fitting a two-way, third order polynomial to gravity readings taken on basement rocks that flank the region (Reilly, 1972; Stern, 1979). This method is widely adopted in New Zealand because the density of the greywacke-schist basement is remarkably uniform at 2670 kg/m^3 (standard deviation of 40 kg/m^3) (Hatherton and Leopard, 1964; Hunt, 1980). The process of separating a residual field from a regional field is subjective and the interpreter's judgement must be used to select the most geologically reasonable regional trend. This usually means selecting the lowest order polynomial fit to the data (Lowrie, 1997). To produce a reasonable representation of the regional field for the CVR, the lowest order polynomial is modelled, only basement rock outside the CVR is used, and the polynomial is constrained by gravity readings to the east, west and south of the region. Some confidence in the residual gravity anomaly values we use can be gained by the fact that the polynomial method used has been applied by different authors in the CVR to produce similar looking maps of residual (Stern, 1979; Rogan, 1982).

In regions of high topographic relief, where the density of the topography differs from the standard reduction density of 2670 kg/m^3, subtle artefacts can be produced by an over or under estimation of terrain effects (Dobrin and Savit, 1988). Relief in the Tokoroa region is extreme in places, with narrow gorges and basins carved into low-

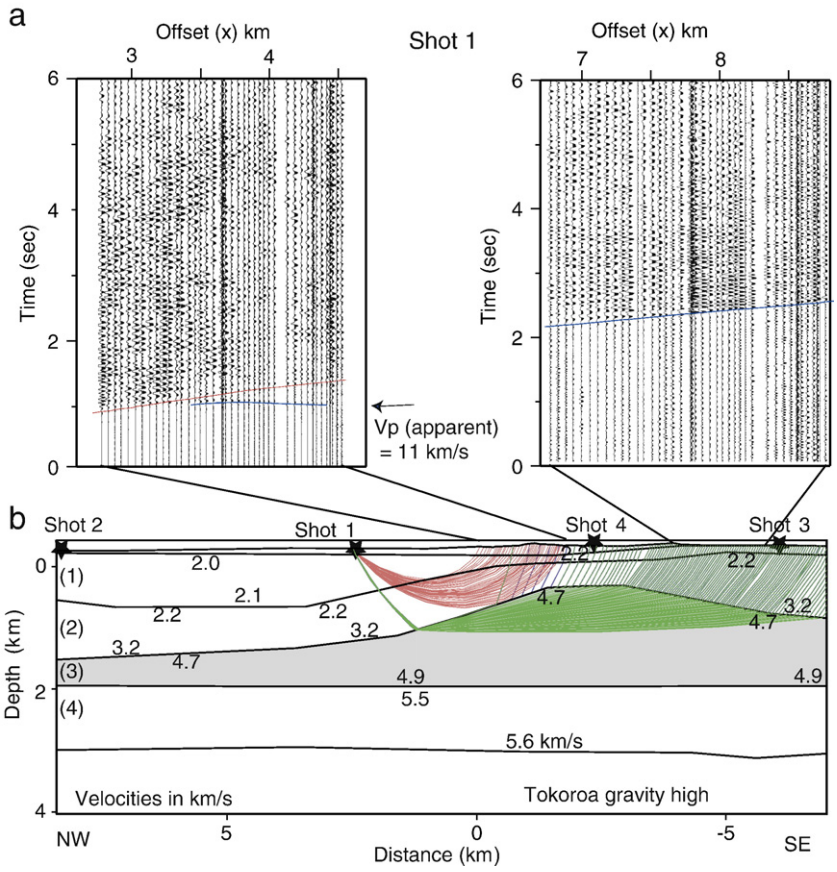

Fig. 6. a). Two 48-channel seismograms for shots of the Tokora-2004 seismic data. Data in seismograms are shown in absolute travel time and spacing between traces is ~50 m. Note the high apparent velocities recorded for arrivals from layer 3. b). Ray-tracing figure for the four shots of the Tokora-2004 seismic data. Top and bottom layer velocities are shown. Offsets are in km and positive to the west. Note the steep slope on the west side to the Tokoroa body (grey shading).

density rhyolitic rock. A rhyolite density of 2100 kg/m^3 is, therefore, used in the reduction of gravity data from the Tokoroa and Mangakino regions.

5.1. Drill hole constraints

There is an overall variation of density for volcanic rocks in the top 2 km of the CVR that can be modelled as an exponential decay of density contrast with depth (Stern, 1986). For example, based on a data set of 2700 borehole wet-density determinations, the predicted density of the volcanic fill will be about 2000 kg/m^3 at the surface and 2540±100 kg/m^3 at a depth of 2000 m (Fig. 7). For an adopted basement density of 2670 kg/m^3, these data suggest that the density contrast between volcanic fill and basement is reduced by 80% at depth of 2 km. Because most drill holes are from the geothermal fields there is some doubt that they are representative as volcaniclastic rocks can be affected by mineralisation of pore spaces (Hochstein and Hunt, 1970). However, when porosity is plotted against depth (Fig. 7b) it can be seen that the increase in density with depth (Fig. 7a) is largely controlled by the collapse of pore space. Both density contrast and porosity decrease by ~88% between the surface and a depth of 2500 m (Fig. 7). Moreover, the exponential coefficient of decrease in porosity with depth (−0.7 km^{-1}) sits within the range of that for shales (−0.5 km^{-1}) and limestones (−0.71 km^{-1}) (Allen and Allen, 2005). Hence the borehole data from the CVR are consistent with compaction under pressure for the volcaniclastic sediments, in a style similar to that for marine sediments.

In the Tokoroa area there are only a few boreholes from which density data are available. Most useful are two holes drilled down to 440 m (Tok-1) (Houghton et al., 1987) and 600 m (HH1) (Allis, 1987) (Fig. 2), on the western and eastern margins, respectively, of the Tokoroa high. The depth range over which density information is common to both drill holes is between 310 and 440 m. Assuming 1-D (i.e. Bouguer slab) structures in the respective holes are representative, the effective difference in residual gravity anomaly (Δg) for the 310–440 m depth range between the two drill holes can be calculated:

$$\text{i.e.} \Delta g = 2\pi G \Delta\rho \Delta h = 0.04193 \Delta\rho \Delta h \quad (2)$$

For $\Delta\rho$ (density contrast) in kg/m^3 and Δh (thickness of Bouguer slab) in km.

Average densities in the calculated depth ranges are 2250 kg/m^3 for Tok-1 and 2010 kg/m^3 for HH1. Thus from Eq. (2) a difference ~1.3 mgal is calculated for $\Delta\rho$=240 kg/m^3 and Δh=0.13 km. If this difference persists over the full ~600 m of volcaniclastics a gravity difference of 6 mgal would be encountered or 24% of the observed residual anomaly of −25 mgal. Thus lateral variations in density within the superficial volcaniclastics could lead to misleading structural interpretations based on residual gravity only. Seismic and borehole data are probably the best means of putting constraints on gravity interpretations in this volcanic environment.

5.2. Gravity modelling techniques

Gravity modelling in three-dimensions is done using methods based on the original equations of Talwani and Ewing (1960). An input structural model consists of several bodies with variable depths and density contrasts (Fig. 8b). An assumed flat surface at 0.4 km above sea

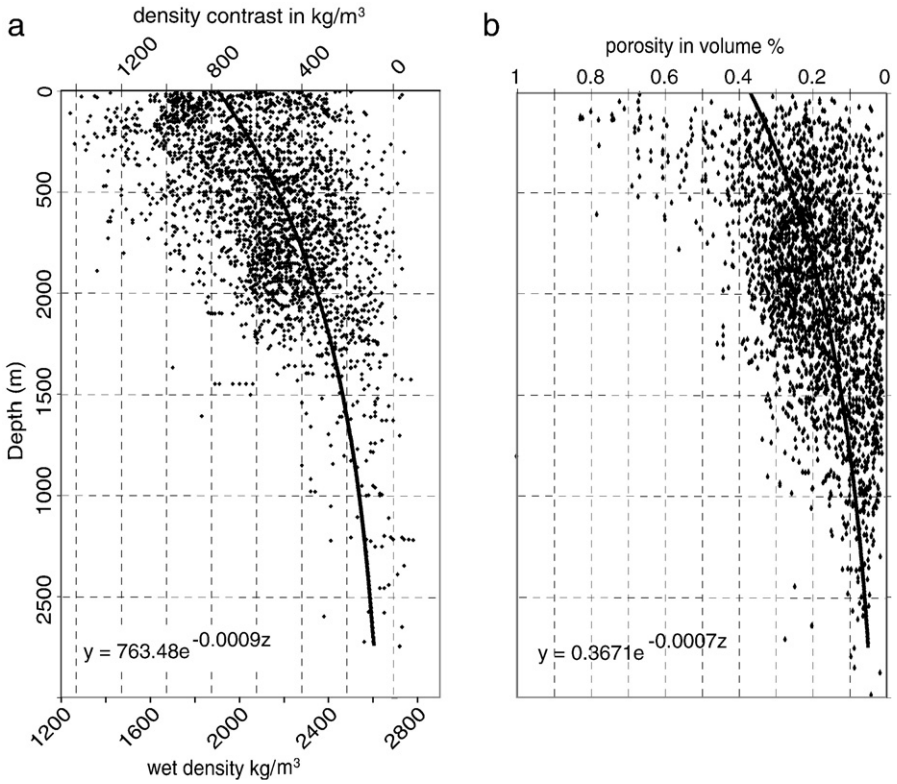

Fig. 7. Density, density contrast (a) and porosity (b) with depth profile for volcanic rocks of the CVR. The Data set, obtained from drill holes, contains 2700 measurements of wet density and porosity from the GNS Science rock database. a.) Data are fit with an exponential decay in density contrast (with respect to a basement density of 2670 kg/m^3) with depth. Although the number of density measurements decreases with depth, scatter in data values also decreases giving an overall exponential decrease in standard deviation and standard error with depth. Density contrast, standard deviation and standard error can thus be estimated from an exponential fit to the data of the form: $Y=A\exp(-bz)$. Where z is depth in metres, and A and b are constants. For density contrast (Y), $A=763.48$ and $b=0.0009$. The standard error on A is 63 and for b is 0.0004 so that at depths (z) of 2500 m and 0 m the standard error is 104 kg/m^3 and 284 kg/m^3, respectively. b). Porosity decreases exponentially with depth, (i.e. depth of burial) as the rocks are progressively squashed by the overburden. The decrease in porosity with depth can be described by the exponential function; Volume percent porosity$=A\exp(-bz)$. Where z is depth in metres, $A=0.3671$ and $b=0.0007$.

level is used to simulate the plane of observations and thus make the model consistent with 2.75D models, which contain topography. Because the 3D modelling is not interactive only the broad wavelengths of the anomaly are fitted: accordingly, an adequate fit is accepted when the residual, R, (observed (Fig. 8a) — predicted (Fig. 8c) is $-3<R<3$ mgals (Fig. 8d).

Additional interactive modelling along the seismic profile lines in 2.75D allows structures to be modelled with strike lengths controlled in and out of the plane of interpretation (Cady, 1980). Higher frequency changes in gravity signature are more readily fitted with 2.75D modelling and an adequate fit is adopted to be where RMS misfits are less than 1.5 mgals.

5.3. Seismic constraints and the meaning of seismic "basement"

From the relationship between seismic velocity (average of 2.0–3.2 km/s velocities and density, an average density contrast of −500 kg/m^3, with respect to regular greywacke rocks, is estimated for the caldera fill. Outside the caldera, cover volcanics are generally modelled with a decreasing density contrast, with respect to basement, with depth (−650 to −200 kg/m^3 from 0–2 km depth) following the analytical function given in Fig. 7. Exceptions to this generalised function do occur within the CVR with the western edge of the Tokoroa gravity high being one area where drill hole data show high densities at shallow depths (Alder, 1989).

It is unclear what rock-type forms seismic basement in the CVR. An assumption made for initial gravity interpretations in the area was that greywacke rocks underlie the entire region (Modriniak and Studt, 1959). Although this assumption is necessary for making a simple gravity model, direct evidence for a pervasive greywacke basement is inconclusive. Just north of Lake Taupo a series of seismic refraction experiments show a P-wave speed of 5.5 km/s is reached at a depth of 2 km (Robinson et al., 1981; Stern, 1986), which is consistent with either greywacke, andesite or compacted volcaniclastics (Sissons and Dibble, 1981). Drilling in the same region intersects highly welded ignimbrite (density=2500 kg/m^3) at this depth and the deepest hole in this region goes down to 2.6 km where the hole terminated in a lower density (2380 kg/m^3) volcanic breccia (Stern, 1987).

In the Mangakino area a recent deep drill hole was put down near the MA-79 seismic line (Fig. 2). Although no density data have been reported, the drill hole terminated at 3.2 km and volcaniclastics were encountered all the way to that depth (Spinks et al., 2005). Other rock types encountered at the base of the deepest drill holes (~2.6–3.0 km) in the CVR are andesite and granodiorite (Stern, 1987; Bowyer, 2005). These rocks have measured densities in the range 2500–2700 kg/m^3 and would have anticipated seismic P-wave velocities of 4.5–5.5 km/s. Thus, there are a variety of different rock types that can be assigned to seismic basement for the CVR.

We model the following beneath 2.2 km in Mangakino Caldera: a layer, between 2.2 and 2.6 km depth, of a density contrast −200 kg/m^3 (with respect to 2670 kg/m^3) to represent the layer of 4.8 km/s velocity or seismic basement as determined by refraction analysis (Fig. 9a). Below the interpreted seismic basement, starting at a depth of ~2.6 km, is 4.0±1 km of sub-basement low-density rock (Fig. 9a). This interpretation is in keeping with results interpreted from the Mangakino seismic array of turning waves through a subsurface low-velocity (hence low-density) body (Fig. 4c). An average seismic velocity of 4.0 km/s is estimated for the body (Eq. (1)), which we

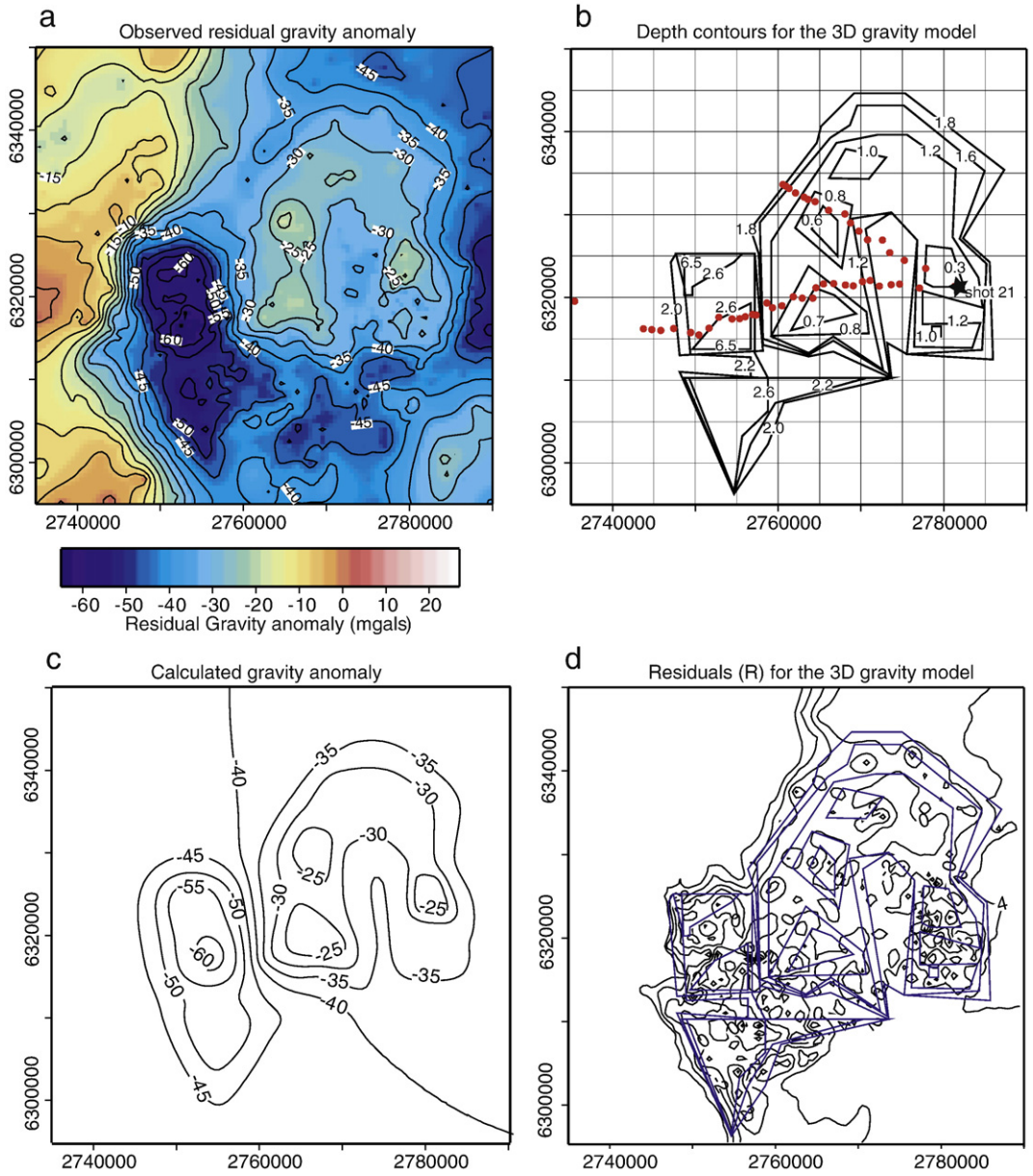

Fig. 8. a.) Contoured residual gravity (reduction density of 2100 kg/m^3) of the Tokoroa and Mangakino areas. b.) Input contours for the 3D gravity modelling algorithm. Numbers are depths below the surface in km. The dots are the Mangakino and Tokoroa seismograph locations and are plotted to indicate the profile lines along which seismic depth constraints are available. c.) Output gravity anomaly from the 3D input structural contours in Fig. 8b. Contours are gravity anomaly in mgals. d.) Observed–modelled residual anomaly for the 3D gravity model. The area beneath the model has residuals (R) of $-3<R<3$ mgals. The contour interval is 1 mgal.

associate with a rock mass of density contrast ~300–400 kg/m^3. There is little variation in density with depth between New Zealand greywacke and the higher grade equivalent schists (Hatherton and Leopard, 1964), so the true density of the deep reaching low-velocity body is inferred to be constant at 2300–2400 kg/m^3.

A rock density of 2500–2600 kg/m^3 for the Tokoroa subsurface "basement" structure provides a satisfactory fit to the data within the uncertainties of seismic depth constraints and reduced gravity anomaly error (~1.5 mgals). This range just captures the lower end for North Island greywacke (Hatherton and Leopard, 1964) and is in the middle of the range for andesites of the Taupo Volcanic Zone (Sissons, 1980).

For the 2.75D model, between 15 and 20 km offset, a density 150 kg/m^3 higher than the topographic density of 2100 kg/m^3 is used for the volcanic cover sequence over the western flank of the Tokoroa high, as drill hole information in this area indicates an increased thickness of welded ignimbrites (Houghton et al., 1987). Volcanic cover rock densities away from this region are modelled in two blocks with 2170 kg/m^3 for the shallow structure and 2270 kg/m^3 for deeper rocks.

5.4. Gravity model interpretations

5.4.1. Tokoroa gravity high

The Tokoroa anomaly is modelled as a 1.2 km deep horseshoe-shaped block of density 2550 kg/m^3 with a central basin (Figs. 8 and 9). On top of the main block, modelled basement highs come to 0.65±0.1, 0.75±0.2 km (with seismic depth constraint) and 1.0 km below the surface along the western flank of the Tokoroa structure (Figs. 8 and 9).

The 1.6 km thickness of low-density volcaniclastics, in the central low of the Tokoroa structure (Fig. 8b) is shallower than the 2.1 km depth determined from seismic constraints and predicted by the

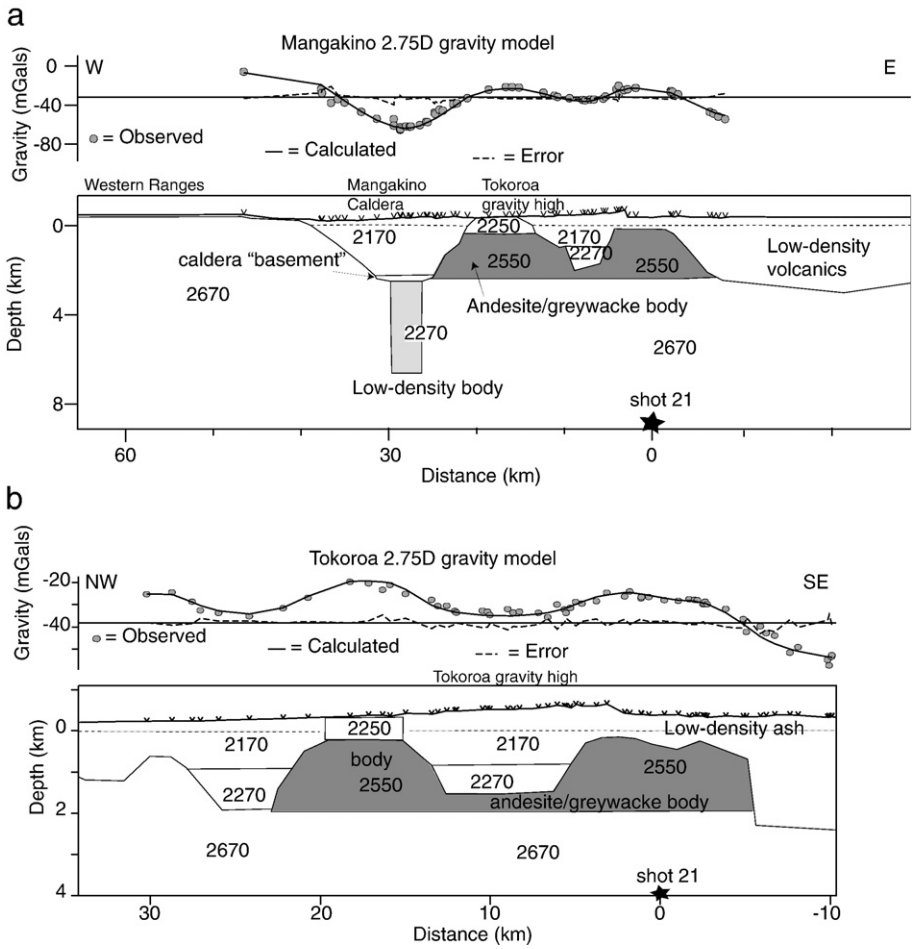

Fig. 9. a.) Gravity model in 2.75D for the Mangakino profile line. The location of the line is shown in Fig. 2. The caldera low-density body is modelled with density contrast of −400 kg/m^3 and is 5 km^2 in surface area. Numbers on the model are densities in kg/m^3 and density contrasts are calculated with respect to a basement of density 2670 kg/m^3. The densities above the dashed line (sea level) are set to zero in the reduction process because the preferred density of volcaniclastics was used in the Bouguer and terrain correction. Below the dashed line blocks have strike lengths in and out of the page of 5 km and are 150 kg/m^3 denser than the background density. Zero offset is at the shot 21 position. b.) Gravity model in 2.75D for the Tokoroa profile. As for the Mangakino profile above. Top of the higher density (andesite/greywacke) body is ~0.65 km below the surface at the west side of the gravity line. Numbers on the model are densities in kg/m^3. Above the dashed line blocks have strike lengths in and out of the page of 5 km and are 150 kg/m^3 denser then the background density.

2.75D gravity model (Figs. 5 and 9). This is possibly a modelling artefact due to the rectangular shape of the model in 3D compared to the V-shaped 2D models.

Trial modelling showed that if a basement structure with a greywacke density of 2670 kg/m^3 was adopted, cover rock of density 2100 kg/m^3 would be required on the western side of the Tokoroa high to fit the seismic and gravity constraints. This is significantly less than densities of volcanic cover rocks as measured from drill hole cores. A mixture of basement rock types, both andesite and greywacke, as seen in the Coromandel (Henrys and Hochstein, 1985) is also possible.

5.4.2. Mangakino gravity anomaly

Two inter-caldera lows, separated by a more positive region are observed on the residual gravity anomaly (Fig. 2) of Mangakino Caldera. These can be modelled as two low-density bodies between 2.6 and 6.5±1 km depth (Fig. 8). Increasing the depth extent of the low-density bodies to greater depths causes larger negative anomalies in the regions just outside, and between, the two lows than observed. These two bodies also need to be relatively small, ~5 km^2 (southern body, 2D and 3D) (Figs. 8 and 9), and ~3 km^2 (northern body, 3D only) in surface area (Fig. 8).

Alternatively, relatively high-density (high-velocity) rocks in the near surface could produce the inter-caldera high. However, these have not been found by the seismic profile running north–south through the basin (Fig. 3) and the model of two distinct low-density bodies at depth is the preferred interpretation.

6. Discussion

6.1. Mangakino Caldera

Due to the small surface area of Mangakino Caldera a large thickness of low-density material is required to model the ~−65 mgals residual anomaly (Fig. 2). Mangakino Caldera has been interpreted as a composite structure (Briggs and McDonough, 1990) and the two sub-basement lows may represent two separate caldera forming, and collapse, events. These collapse events are most likely to have occurred during an intense period of caldera forming eruptions from 1.23 Ma to 0.91 Ma. Three large volume (>300 km^3) ignimbrites were erupted during this period (Briggs et al., 1993).

Deep reaching low-density bodies beneath calderas are common. For example, residual gravity anomalies beneath calderas in the Rocky Mountains, Nevada (Lipman, 2007) and the Alto Plano of the Andes (de Silva and Gosnold, 2007), have been interpreted as due to low-density bodies to depths of ~10 km. These bodies are inferred to be granite–granodiorite plutons (Lipman, 2007) implying densities ranging from 2600–2800 kg/m^3 (Christensen and Mooney, 1995). This interpretation will not, however, work for the caldera structures

beneath the central North Island. Here the basement greywacke rocks found each side of the volcanic region have densities close to that reported for granites and granodiorites (~2600–2700 kg/m^3), and therefore negative residual gravity anomalies have to be accounted for rocks with densities less than this.

The inferred seismic velocity and density ranges of the anomalous body beneath Mangakino Caldera are 4 km/s and 2300–2400 kg/m^3 respectively. Such a density range is too low to be attributable to a regular cooled igneous intrusion and thus Mangakino Caldera still remains an enigma. The simplest explanation of the −65 mgal gravity anomaly is a ~6.5 km thickness of low-density volcaniclastic rocks that have back-filled an explosive vent. But how such a large thickness of low-density, low-velocity volcanics is sustained for ~1 My is not clear. Compaction from overburden pressure should expel most of the porosity and, based on drill hole evidence (Fig. 7b) from elsewhere within the CVR (Stern, 1987), the density contrast of the volcanic fill with basement should virtually have vanished by a depth of 2.5–3 km.

One possible way to sustain the porosity, and hence low densities in the back-filled volcanics is that high fluid pressure within the deep volcanic edifices are inhibiting compaction and hence densification of the volcanic fill. High fluid pressures could be sustained in the deep low-density bodies if a seal, such as a highly welded ignimbrite flow, was emplaced over the top of the edifices after they had been partly back-filled, and injection of volatiles and/or melts into the caldera continued at depth. Moreover, in hydrothermal zones, such as Mangakino Caldera, self-sealing processes in fractures are common and mineralised fractures (veins) may act as barriers to fluid flow (Tenthorey et al., 2003). I.e. for any crack or joint within the caldera sequence the effective stress ($\bar{\sigma}_{ij}$) across the interface is given by:

$$\bar{\sigma}_{ij} = \sigma_{ij} - P\delta_{ij} \tag{3}$$

Where σ_{ij} is the applied stress of the lithostatic column, P is the fluid pressure and δ_{ij} is a Kronecker delta (Scholz, 1990). Thus, as P approaches the pressure of the overburden (i.e. lithostatic pressure), the porosity of volcanic sequence, and hence density, approaches that of near surface equivalent values. For this sequence of events to be viable, however, it is vital that lower volcanic sequence becomes sealed and pressurised soon after emplacement and is sustained there after.

Evidence for a similar deep-seated, volcanic sequence beneath a recently active caldera came from a seismic-gravity profile across the north end of Lake Taupo (Stern, 1986) (Fig. 2). Here the minimum residual gravity anomaly is −55 mgals yet the volcanic cover sequences above the 2 km deep seismic basement can only account for −35 to −40 mgals of the anomaly. The second-order residual anomaly of −15 mgals was also attributed to a sub-basement low-density body extending to depths of around ~4 km (Stern, 1986). A drill hole has penetrated the full sequence here and shows an apparent inversion of densities at about 2.4 km, albeit based on a single sample at this depth.

6.2. The Tokoroa gravity high

Subsurface structure at Tokoroa is important for two reasons. Firstly, from a resource exploration viewpoint there has been past interest in the Tokoroa area where electrical surveying has shown promising hydrothermal mineralisation (Allis, 1987). If the source of the gravity high is a volcanic structure then the potential for widespread mineralisation in the subsurface is enhanced. Secondly, if the Tokoroa subsurface structure is volcanic, then its geophysical properties point strongly to it being a buried andesite massif with a size and volume similar to that of the Tongariro Volcanic Complex at the southern most apex of the CVR (Fig. 1). If the structure is a remnant volcanic centre, how does it fit into a conceptual model for the CVR? It could be viewed in two ways: an andesite massif that marks the southern end of the Hauraki–Coromandel trend which was active before the switch to the development of the NE–SW orientated Taupo Volcanic Zone (Wilson et al., 1995); or a massif that was the southern apex of the volcanic zone at ~2–3 Ma and thus represents a part of the continuous rotation and translation of volcanism through central North Island (Stern et al., 2006).

Although the shape of the subsurface structure beneath Tokoroa is perhaps more consistent with a buried volcanic complex (Fig. 8), we cannot rule out a non-volcanic model with the geophysical data presented here. The key contribution of this paper is, however, to highlight the existence and scale of these impressive subsurface structures within the central North Island, and point out the potential importance of drilling to and sampling the subsurface body.

7. Conclusions

The conclusions of this study are:

1. Seismic refraction methods from large (~100–1000 kg) dynamite shots can be used as effective constraints for the gravity interpretation of rhyolitic caldera structures. Lower frequency signal inherent in refraction data do not suffer attenuation to the same degree as seismic reflection data.
2. In the caldera structures of the Central Volcanic Region of New Zealand several calderas exhibit residual gravity anomalies <−55 mgal. High seismic velocities at ~2 km depth and densities from borehole data show that density inversions are required at depths of 2.5–6.5±1 km to explain the gravity data. In the case of the Mangakino Caldera there are high-amplitude, seismic refraction, second arrivals that are most readily interpreted as waves that have been channelled through a low-velocity body directly beneath the caldera.
3. We speculatively interpret the deeper caldera structure as a seismic velocity and density inversion linked to high fluid pressures associated with on going volcanic and/or geothermal activity.
4. The causative structure associated with the Tokoroa gravity high is imaged with seismic refraction methods. It appears to be a broad 20 km×20 km platform on top of which are three prominent peaks. From the form and properties of the imaged structure we interpret the causative structure to be an old volcanic centre the top of which is about 650 m below the surface. The dimensions of the subsurface structure are similar to that of the presently active Tongariro Volcanic Complex at the southern apex of the Central Volcanic Region.
5. Both the Mangakino and Tokoroa structures are critically placed at the hinge point between late Miocene and late Pliocene volcanic arcs of the North Island. Drilling and dating the Tokoroa structure would, providing that it is a volcanic structure, give a strong lead on how volcanism, and hence the plate boundary, migrated through and beneath this active continental margin.

Acknowledgments

We thank two anonymous referees for their constructive reviews of an initial version of this paper. Data acquisition was funded by the New Zealand Foundation for Science and Technology, and collected as part of the NIGHT (North Island GeopHysical Transect) project. We gratefully acknowledge the assistance of the NIGHT team, including workers from institutions in New Zealand, the U.K and Japan. Victoria University Research Grant VIC5033 funded data acquisition for the Tok-2004 seismic array. Special thanks to the staff and students from the Institute of geophysics, Victoria University who assisted in the field campaign. W.R. Sratford was supported by a TIFF PhD Scholarship from the New Zealand Science Foundation and GlassEarthGold LTD.

References

Alder, G.F., 1989. Seismic and gravity studies of the Tokoroa gravity anomaly, North Island, New Zealand. MSc Thesis, Victoria University, Wellington, New Zealand.

Allen, P.A., Allen, J.R., 2005. Basin Analysis: Principles and Applications. Blackwell Publishing.

Allis, R.G., 1987. Geophysical and Geochemical Investigations of the Horohoro Geothermal Prospect. Geophys. div., DSIR, Wellington, NZ.

Blank, H.R., 1965. Ash-flow deposits of the central King Country, New Zealand. N.Z. J. Geol. Geophys. 8, 588–607.

Bowyer, D., 2005. Results of recent drilling at Rotokawa, Proceedings NZ Geothermal Workshop, Rotorua.

Briggs, R.M., 1986. Volcanic rocks of the Waikato region, western North Island, and some possible petrologic and tectonic constraints on their origin. Late Cenozoic Volcanism in New Zealand. R. Soc. N.Z. 23, 76–91.

Briggs, R.M., McDonough, W.F., 1990. Contemporaneous convergent margin and intraplate magmatism, North Island, New Zealand. J. Petrol. 31, 813–851.

Briggs, R.M., Gifford, M.G., Moyle, A.R., Taylor, S.R., Norman, M.D., Houghton, B.F., Wilson, C.J., 1993. Geochemical zoning and eruptive mixing in ignimbrites from Mangakino volcano, Taupo Volcanic Zone, New Zealand. J. Volcanol. Geotherm. Res. 56, 175–203.

Briggs, R.M., Lowe, D.J., Esler, E.R., Smith, R.T., Henry, M.A.C., Wehrmann, H., Manning, D.A., 2006. Geology of the Maketu Area, Bay of Plenty, North Island, New Zealand, Department of Earth and Ocean Sciences, University of Waikato, Hamilton, New Zealand.

Cady, J.W., 1980. Calculation of gravity and magnetic anomalies of finite length right polygonal prisms. Geophysics 45, 1507–1512.

Calhaem, I.M., 1973. Asymmetric spreading from a volcanic arc to an active continental margin, Dept. Phys. Rep. 8/73. Victoria University, Wellington, New Zealand, p. 8.

Carter, L., Shane, P., Alloway, B., Hall, I.R., Harris, S.E., Westgate, J.A., 2003. Demise of one volcanic zone and birth of another—a 12 m.y. marine record of major rhyolitic eruptions from New Zealand. Geology 31 (6), 493–496.

Christensen, N.I., Mooney, W.D., 1995. Seismic velocity structure and composition of the continental crust: a global review. J. Geophys. Res. 100 (B7), 9761–9788.

Cole, J.W., Lewis, K.B., 1981. Evolution of the Taupo–Hikurangi subduction system. Tectonophysics 72, 1–21.

Cole, J.W., Darby, D.J., Stern, T.A., 1995. Taupo Volcanic Zone and Central Volcanic Region: Backarc structures of North Island, New Zealand. In: Taylor, B. (Ed.), Backarc Basins. Plenum Press, New York, pp. 1–28.

de Silva, S., Gosnold, W.D., 2007. Episodic construction of batholiths: insights from the spatiotemporal development of an ignimbrite flare-up. J. Volcanol. Geotherm. Res. 167 (1–4), 320–335.

Dobrin, M.B., Savit, C.H., 1988. Introduction to Geophysical Prospecting, Forth edition. Mcgraw-Hill Book Company, New York.

Faccenna, C., Becker, T.W., Pio Lucente, F., Jolivet, L., Rossetti, F., 2001. History of subduction and back-arc extension in the central Mediterranean. Geophys. J. Int. 145, 809–820.

Farmer, G.L., Glazner, A.F., Manley, C.R., 2002. Did lithospheric delamination trigger late Cenozoic potassic volcanism in the southern Sierra Nevada, California? Geol. Soc. Am. Bull. 114, 754–768.

Grindley, G.W., Mumme, T.C., 1991. Magnetic stratigraphy and correlation of ignimbrite eruptions of the Mangakino Basin and Tokoroa Plateau. N.Z. Geol. Surv. Rec. 43, 25–36.

Hamilton, W.B., 1995. Subduction systems and magmatism. Geol. Soc. London Spec. Pub. 81, 3–28.

Hatherton, T., 1969. The geophysical significance of calc-alkaline andesites in New Zealand. N. Z. Geol. Geophys. 12, 436–459.

Hatherton, T., Leopard, A.E., 1964. The densities of New Zealand rocks. N.Z. Geol. Geophys. 7, 605–625.

Healy, J., Schofield, J.C. and Thompson, B.N., 1964. Sheet 5 — Rotorua. Geological map of New Zealand. N.Z. Geol. Sur.

Henrys, S.A., Hochstein, M.P., 1985. A geophysical reconnaissance survey of Great Barrier Island, North Island, New Zealand. N.Z. Geol. Geophys. 28, 383–396.

Henrys, S.H., Reyners, M., Bibby, H., 2003. Exploring the plate boundary structure of the North Island, New Zealand. Eos. Trans. AGU 84, 289–295.

Hochstein, M.P., Hunt, T.M., 1970. Seismic, gravity and magnetic studies, Broadlands geothermal field, New Zealand. Geothermics 2, 333–346.

Hochstein, M.P., Ballance, P.F., 1993. Hauraki rift: a young, active, intra-continental rift in a bark-arc setting. Sedimentary Basins of the World, South Pacific Sedimentary Basins. Chapter 17. Elsevier Science Publishers, Amsterdam, pp. 295–305.

Horgan, H., 2003. The thermal and crustal structure of a continental back-arc basin: offshore Bay of Plenty, New Zealand. MSc Thesis, Victoria University, Wellington, New Zealand.

Houghton, B.F., Wilson, C.J.N., Stern, T.A., 1987. Ignimbrite stratigraphy of a 457 M deep drillhole near Tokoroa. N.Z. Geol. Surv. Rec. 20, 51–55.

Hunt, T.M., 1980. Basement structure of the Wanganui Basin, onshore, interpreted from gravity data. N.Z. Geol. Geophys. 23, 1–16.

Issac, M.J.R., Herzer, R.H., Brook, F.J., Hayward, B., 1994. Cretaceous and Cenozoic geology of Northland, New Zealand. Inst. Geol. Nucl. Sci., Monogr. 8.

King, P., 2000. Tectonic reconstructions of New Zealand: 40 Ma to the present. N.Z. Geol. Geophys. 43, 611–638.

Krippner, S.J.P., Briggs, R.M., Wilson, C.J.N., Cole, J.W., 1998. Petrography and geochemistry of lithic fragments in ignimbrites from the Mangakino Volcanic Centre: implications for the composition of the subvolcanic crust in western Taupo Volcanic Zone, New Zealand. N.Z. J. Geol. Geophys. 41, 187–199.

Lipman, P.W., 2007. Incremental assembly and prolonged consolidation of Cordilleran magma chambers: evidence from the Southern Rocky Mountain volcanic field. Geosphere 3 (1), 42–70.

Lowrie, W., 1997. Fundamentals of Geophysics. Cambridge University Press, Cambridge.

Modriniak, N., Studt, F.E., 1959. Geological structure and volcanism of the Taupo–Tarawera district. N.Z. Geol. Geophys. 2, 654–684.

Murase, T., McBirney, A.R., 1973. Properties of some common igneous rocks and their melts at high temperatures. Bull. Geol. Soc. Am. 84 (M-33), 3563–3592.

Nicol, A., Mazengarb, C., Chanier, F., Rait, G., Uruski, C., Wallace, L., 2007. Tectonic evolution of the active Hikurangi subduction margin, New Zealand, since the Oligocene. Tectonics 26, 10.1029.

Reilly, W.I., 1972. New Zealand gravity map series. N. Z. J. Geol. Geophys. 15 (1), 3–15.

Robinson, R., Smith, E.G.C., Latter, J.H., 1981. Seismic studies of the crust under the hydrothermal areas of the Taupo Volcanic Zone N.Z. J. Volcanol. Geotherm. Res. 9, 253–267.

Rogan, A.M., 1982. A geophysical study of the Taupo Volcanic Zone, New Zealand. J. Geophys. Res. 87, 4073–4088.

Salmon, M., Savage, M., Stern, T., Stratford, W., 2004. Geophysical observations of processes in the mantle wedge, central North Island New Zealand., Presented at the Geo3 Conference, 2004, Taupo, New Zealand.

Scholz, C.H., 1990. The Mechanics of Earthquakes and Faulting. Cambridge University Press, Cambridge, p. 439.

Sheriff, R.E., Geldart, L.P., 1995. Exploration seismology. Cambridge University Press, p. 592.

Sissons, B.A., 1980. Densities determined from surface and subsurface gravity measurements. Geophysics 46, 1568–1571.

Sissons, B.A., Dibble, R.R., 1981. A seismic refraction experiment southeast of Ruapehu volcano. N.Z. J. Geol. Geophys. 24, 31–38.

Skinner, D., 1986. Neogene volcanism of the Hauraki Volcanic Region. Late Cenozoic volcanism in New Zealand. R. Soc. N.Z. Bull. 23, 21–47.

Spinks, K., Urzua, L., Cumming, B., Bowyer, D., 2005. The geology and geothermal exploration of Mangakino Caldera, New Zealand Geothermal Workshop, Rotorua.

Stern, T.A., 1979. Regional and residual gravity fields, central North Island, New Zealand. N.Z. J. Geol. Geophys. 22 (4), 479–485.

Stern, T.A., 1982. Seismic and gravity investigations of the Central Volcanic Region, North Island, New Zealand. PhD Thesis, Victoria University, Wellington, New Zealand.

Stern, T.A., 1986. Geophysical studies of the upper crust within the Central Volcanic Region, New Zealand. Late Cenozoic Volcanism in New Zealand. R. Soc. N.Z. Bull. 23, 92–111 Wellington.

Stern, T.A., 1987. Asymmetric back-arc spreading, heat flux and structure associated with the Central Volcanic Region of New Zealand. Earth Planet. Sci. Lett. 85, 265–276.

Stern, T.A., Stratford, W.R., Salmon, M.L., 2006. Subduction at a continental margin: kinematics and dynamics of the central North Island, New Zealand. Rev. Geophys. 44 (4). doi:10.1029/2005RG000171.

Stipp, J.J., Thompson, B.N., 1971. K/Ar ages from the volcanics of North Island, New Zealand. N.Z. J. Geol. Geophys 14, 403–413.

Stoneley, R., 1968. A lower Tertiary decollement on the East Coast, North Island, New Zealand. N.Z. J. Geol. Geophys. (11), 128–156.

Stratford, W.R., Stern, T.A., 2006. Crust and upper mantle structure of a continental backarc: central North Island, New Zealand. Geophys. J. Int. 166, 469–484.

Talwani, M., Ewing, E., 1960. Rapid computation of gravitational attraction of three-dimensional bodies of arbitrary shape. Geophysics 25 (1), 203–225.

Tenthorey, E., Cox, S., Todd, F.F., 2003. Evolution of strength recovery and permeability during fluid–rock reaction in experimental fault zones. Earth Planet. Sci. Lett. 206, 161–172.

Wallace, L.M., Beaven, J., McCaffrey, R., Darby, D., 2004. Subduction zone coupling and tectonic block rotations in the North Island, New Zealand. J. Geophys. Res. 109 (B12406), 1–21.

Wilson, C.J.N., 1986. Reconnaissance stratigraphy and volcanology of ignimbrites from Mangakino Volcano. In: Smith, I.E.M. (Ed.), Late Cenozoic Volcanism. R. Soc. of NZ.

Wilson, C.J.N., Houghton, B.F., McWilliams, M.O., Lanphere, M.A., Weaver, S.D., Briggs, R.M., 1995. Volcanic and structural evolution of the Taupo Volcanic Zone, New Zealand: a review. J. Volcanol. Geotherm. Res. 68, 1–28.

Wright, I.C., Walcott, R.I., 1986. Large tectonic rotation of part of New Zealand in the last 5 Ma. Earth Planet. Sci. Lett. 80, 348–352.